Stability Of Open-Cycle Radial-Inflow Disk Generators

Author(s): S. M. Marty, S. W. Simpson, and H. K. Messerle

Session Name: Generators B

SEAM: 28 (1990)

SEAM EDX URL: https://edx.netl.doe.gov/dataset/seam-28

EDX Paper ID: 1432

STABILITY OF OPEN-CYCLE RADIAL-INFLOW DISK GENERATORS

S.M. Marty, S.W. Simpson and H.K. Messerle

School of Electrical Engineering,
University of Sydney, N.S.W., Australia.

ABSTRACT

The stability of the open-cycle radial-inflow disk generator under conditions relevant to base-load operation has been investigated by numerically solving the fluid flow equations with time dependence included. Results of linear perturbation analysis are also presented. It is shown that the generator may be subject to magnetoacoustic instabilities despite operation in the subsonic regime. The results indicate that the generator operates in a region of marginal stability and a reduction in the combustion temperature or the magnetic field strength produces stable operation, although at the expense of reduced enthalpy extraction. It may also be possible to stabilize operation of the inflow disk with additional control electrodes.

INTRODUCTION

The simplicity of the disk generator configuration, which requires fewer electrodes and has a simpler, less costly magnet, has made it an attractive alternative to linear generators. In a previous theoretical study of the disk generator, the performance of various design cases was analysed.[1] These design cases predicted the optimum performance achievable for a particular flow configuration given the generator's operating parameters: magnetic field strength, transport properties, thermal input etc. The calculations showed that the most promising configurations were the supersonic radial outflow with radial electric field held constant, and the subsonic radial inflow generator with the Mach number held constant. In the case of the inflow generator with subsonic flow, detailed steady-state analyses, both in one dimension[2] and two dimensions[3] have indicated that, in terms of enthalpy extraction, the performance is comparable to that of the linear generator with diagonal connection. However, it is important to know how the generators will behave away from their design point and how they will respond to load or flow transients. Also, since the disk generator is basically a Hall generator, it is necessary to investigate the possibility that the disk is unstable to magnetoacoustic waves, which theory has shown could alter the global state of linear Hall generators.[4,5] In this paper, the effects of magnetoacoustic waves on the inflow generator are studied.

In previous studies, both one and two-dimensional ($r-\theta$) time-dependent models of the plasma flow, in addition to a perturbation analysis, have shown that the supersonic radial outflow generator is likely to be subject to severe magnetoacoustic instabilities.[6,7] Growth times for base-load outflow disk designs are of the order of 0.5 ms, and once the instability is established, the generator flow conditions move away from the design state. In some cases, a shock front propagates upstream in the channel, and in others, unacceptably high electric field stresses are set up along the channel.

The possibility of stabilizing the outflow disk generator by the use of additional control electrodes has also been investigated.[6] Control electrodes were proposed by Retallick et al.[8] in order to alleviate problems associated with the steep V-I characteristic of the outflow disk generator. In fact, the steep V-I load curves calculated under some conditions[8] were a reflection of the fact that the generator is unstable to the magnetoacoustic wave. Several circuit configurations were examined; however, it was found that, with a practical number of control electrodes, the outflow disk could not be stabilised for design conditions corresponding to optimum enthalpy extraction.[6]

From the two-dimensional study,[7] it was found that the boundary conditions at the electrodes, viz. $E_\theta=0$, are sufficient to prevent significant flow nonuniformities developing in the θ-direction. In this situation, the gradients in the θ-direction are negligible and the one-dimensional analysis accurately reflects generator behaviour.

In the present study, a one-dimensional model is used to investigate the stability of a radial-inflow generator operating under conditions which would be likely in base-load applications. In order to provide a comparison with the results for the outflow generator,[6,7] the same combustor conditions and magnetic field strength were chosen for the design calculations. These parameters were originally used in the previous disk generator study carried out for NASA.[8] The design selected in Ref. 2 employed similar combustor properties but a higher magnetic field strength than that chosen here and would be expected to be at least as unstable as the generator design studied in this paper.

GOVERNING EQUATIONS AND NUMERICAL MODEL

Gasdynamic Equations

The governing equations for the gasdynamic properties are:

$$\frac{\partial\rho}{\partial t} + \nabla\cdot(\rho v) = 0 \tag{1}$$

$$\rho\left(\frac{\partial}{\partial t} + v\cdot\nabla\right)v = -\nabla p + J\times B \tag{2}$$

$$\rho\left(\frac{\partial}{\partial t} + v\cdot\nabla\right)\left(h + \frac{v^2}{2}\right) = \frac{\partial p}{\partial t} + J\cdot E \tag{3}$$

In equations (1)-(3), wall friction and heat loss are neglected. The symbols have their usual meanings.

For their numerical solution, equations (1)–(3) are written in conservation form. In this form the independent variables are the mass density ρ, radial momentum density $m_r = \rho v_r$, azimuthal momentum density $m_\theta = \rho v_\theta$, and the total energy density $e = \rho[e + (v_r^2+v_\theta^2)/2]$ where e is the internal energy per unit volume. Cylindrical coordinates are used.

The conservation equations can be expressed in "vector" form, where the vectors $\underline{U}$, $\underline{F}_r$, $\underline{C}$, $\underline{H}$ and $\underline{S}$ are ordered sets of the equations' terms. The one-dimensional form is

$$(\underline{U})_t = -(\underline{F}_r)_r - \frac{1}{r}\underline{C} - \underline{H} + \underline{S} \tag{4}$$

where:

$$\underline{U}(r,t) = \begin{bmatrix} \rho \\ m_r \\ m_\theta \\ e \end{bmatrix}$$

describes the fluid state,

$$\underline{F}_r = \begin{bmatrix} m_r \\ m_r^2/\rho + p \\ m_r m_\theta/\rho \\ (e + p)\, m_r/\rho \end{bmatrix}$$

describes the mass, momentum and energy fluxes in the radial direction;

$$\underline{C} = \begin{bmatrix} 0 \\ m_\theta^2/\rho \\ -m_r m_\theta/\rho \\ 0 \end{bmatrix}$$

gives the centrifugal force terms;

$$\underline{H} = A^{-1}(A)_r \begin{bmatrix} m_r \\ m_r^2/\rho \\ m_r m_\theta/\rho \\ (e + p)\, m_r/\rho \end{bmatrix}$$

describes the area variation effect; and

$$\underline{S} = \begin{bmatrix} 0 \\ J_\theta B \\ -J_r B \\ -J_r E_r \end{bmatrix}$$

contains the Lorentz force and joule dissipation terms.

A further assumption is that both the isentropic exponent, γ, and the specific heat at constant pressure, C_p, are constants. Employing this assumption significantly reduces the computational time. The equation of state may then be expressed as

$$p = (\gamma - 1)\left(e - \frac{m^2}{2\rho}\right) \tag{5}$$

where $m^2 = m_r^2 + m_\theta^2$.

The vector equation (4) may be rewritten as

$$(\underline{U})_t = -[\underline{F}_r(\underline{U})]_r + \underline{D}(\underline{U},r,t) \tag{6}$$

where

$$\underline{D}(\underline{U},r,t) = -\underline{H}(\underline{U},r,t) + \underline{S}(\underline{U},r,t) - \underline{C}(\underline{U},r,t)/r$$

To solve equation (4) numerically, the partial derivative operators in time and space are replaced by non-linear finite difference operators. The space and time co-ordinates are discretised with finite differences δr and δt such that

$$r = i\delta r$$
$$t = n\delta t$$

where i, and n are integers. The method used in the calculations is the two-step method of McCormack[9] which alternately takes forward and backward differences for the two steps. The two-step operator is formed by first calculating an intermediate state $\underline{U}^*$, where

$$\underline{U}^* = \underline{U}^n - \frac{\delta t}{\delta r}\Delta_r^+ \underline{F}_r(\underline{U}^n) + \delta t\, \underline{D}(\underline{U}^n) \tag{7}$$

The final state is

$$\underline{U}^{n+1} = 0.5 \times [\underline{U}^n + \underline{U}^* - \frac{\delta t}{\delta r}\Delta_r^- \underline{F}_r(\underline{U}^*) + \delta t\, \underline{D}(\underline{U}^*)] \tag{8}$$

The forward and backward difference operators are defined by

$$\Delta_r^+ f(r) = f(r + \delta r) - f(r)$$

$$\Delta_r^- f(r) = f(r) - f(r - \delta r)$$

Boundary Conditions and Initial State

An analysis of unsteady MHD channel flow involves the specification of an initial fluid state $\underline{U}(r,0)$. For a given scheme of electrical loading and boundary conditions, the fluid states subsequent to the initial state are then computed. The boundary conditions require the specification of the fluid states $\underline{U}(r_i,t)$ and $\underline{U}(r_o,t)$, where r_i and r_o are the inlet and outlet radii of the channel. The initial fluid state may be obtained by numerically solving the one-dimensional steady flow equations to calculate the flow variables at t=0 and the channel area profile. In solving the flow equations here, the constraint of constant Mach number is used. The pressure at the exit of the generator is matched to the diffuser outlet pressure through a normal shock with an assumed diffuser efficiency of 0.7. It is assumed that the combustor conditions remain constant and that the expansion fom the combustor to the channel inlet is isentropic.

The very steep operating characteristic obtained from a steady-state analysis of the open-cycle disk generator indicates that the generator approximates a constant current device.[8] For the calculations here, the current is held constant. In calculations of the time-dependent behaviour of outflow disk generators, it was found that stability could not be significantly improved with simple load circuits consisting of resistors and inductors connected in series.[6]

RESULTS

The operating conditions for the inflow disk were chosen to be comparable to those used in previous studies of the outflow disk.[6-8] The operating conditions at the design point are given in Table 1. The microscopic Hall parameter and electrical conductivity were calculated assuming chemical equilibrium. Two load circuits are used for improved load matching, as shown in Figure 1, with the intermediate electrode located at a radius of 3.0 m.

At the operating point, the steady analysis predicts that an enthalpy extraction of 18.8% would be achieved. Once the initial channel flow conditions were set up using the steady state model, the time-dependent model was used to follow the development of any possible instabilities. In Figure 2, the difference in the value of the electric field strength from its value at t=0 is shown versus channel radius for times of 2, 3 and 4 msec after the start of calculations. It can be seen from Figure 2 that the inflow disk generator is in fact unstable, with oscillations appearing along the channel as a result of perturbations caused by numerical imprecision in the computer calculations. The oscillation in the electric field which is evident in Figure 2 has the properties of the magnetoacoustic instability, that is, a wave propagating upstream at approximately the sonic velocity with respect to the flow.

By measuring the growth of the electric field when the fluctuations are just beginning to appear, it is possible to estimate the growth time constant,[6] which is approximately 2.2 msec. Figure 3 shows the electric field strength versus channel radius for a comparable outflow disk generator design.[6] Profiles are shown for times 2.2, 2.4, and 2.6 msec after the start of calculations. Comparing Figures 2 and 3, it can be seen that the growth rate is much higher for the outflow geometry. From the data plotted in Figure 3, the growth time constant is found to be 0.4 msec for the outflow disk generator.[6]

In both Figures 2 and 3, it can be seen that wave growth is greatest in the downstream part of the channel. For the inflow geometry (Figure 2), this is a consequence of the higher values of Hall parameter in that section of the channel. In the design case, the Hall parameter rises from 1.9 at the channel inlet to 6.8 at the outlet. For the outflow geometry, the Mach number is close to unity near the channel outlet and this leads to rapid growth of the instability. In Figures 2 and 3, wave motion can be observed from the displacement of the extrema in the waveform with time. The magnetoacoustic wave travels at close to sonic velocity with respect to the flow, resulting in the wave moving upstream in the inflow disk channel (Figure 2) and downstream in the outflow disk channel (Figure 3).

The effect of perturbing the load current in the downstream portion of the channel (Load Current 2 in Table 1) from its design value was also investigated. When the current is greater than the design value, the flow in the channel accelerates with instabilities similar to those shown in Figure 2 developing. Eventually numerical instabilities prevent further computation. When the current is reduced below the design value, the behaviour is qualitatively different: a new, stable operating state is obtained. The new state is characterized by a much reduced Mach number and a higher pressure along the channel. In Figure 4, the Mach number is shown versus radius at 10 msec intervals after t=0. After 40 msec, the flow is close to its final steady state. For this calculation, the current in load circuit 2 was reduced by 0.5% from its design value. It is clear that the new state is very different to the design case: the enthalpy extraction of a generator operating under these conditions is reduced to unacceptably low values, making this particular design impractical.

Fuel	Montana Rosebud (2% moisture)
Oxidiser	Preheated Air
Magnetic Field (tesla)	7.0
Thermal Input (MW)	2000
Channel Inlet Conditions	
P_{tot} (atm)	5.53
T_{tot} (K)	2833
Mach no.	0.9
Swirl	2.0
Radius (m)	4.50
Channel height (cm)	15
Channel Exit Conditions	
Diffuser efficiency	0.7
Diffuser exit pressure (atm)	1.15
Exit radius (m)	1.85
Channel height at exit (cm)	67
Load Current 1 (kA)	46.0
Load Current 2 (kA)	34.0

Table 1. Operating Conditions at the design point.

When either the temperature in the channel, the magnetic field strength or the Mach number are reduced, the tendency is towards improved stability. If the combustor temperature is lowered to 2770 K, keeping the magnetic field and Mach number at their design values, then the flow is stable under design conditions. For this case, the first and second load circuit currents are 32 and 17 kA respectively and the enthalpy extraction is reduced to 16.4%. With the design criterion of constant Mach number, and with the combustor temperature maintained at its design value, a stable state could also be obtained by reducing the magnetic field strength to 5.5 tesla, although again at the expense of reduced enthalpy extraction.

If the Mach number is reduced, the channel tends towards stability with the growth time and wavelength of the instability increased. However, with the channel inlet radius specified in Table 1, an initial state that was stable could not be produced by the design code. The lower interaction in the channel meant that the diffuser boundary condition could not be matched at a practical outlet radius.

A perturbation analysis of the one-dimensional equations describing the inflow disk has also been carried out. The method, which applies equally to the inflow or outflow configurations, is described in detail in Ref. 6. Using the flow properties of the inflow generator at the channel mid-radius, for the design case parameters given in Table 1, a growth time of 1.9 msec is calculated for magnetoacoustic waves. This is in reasonable agreement with the result obtained with the non-linear analysis (2.2 msec). In Figure 5, the growth time is shown versus Mach number for the magnetoacoustic wave using the mid-channel properties. The trend is towards longer growth times as the Mach number is reduced, in agreement with the non-linear analysis.

Figure 5 also illustrates that for supersonic channels wave growth is more rapid, in agreement with the observation that the outflow disk generator is more unstable (see Figures 2 and 3).

In Figure 6, the growth time is shown versus magnetic field strength, again calculated with the mid-channel properties. A reduction in the field strength increases the growth time, as also predicted by the non-linear calculation. This dependence on magnetic field, and hence Hall parameter, is also consistent with the observation that wave growth is first seen near the channel exit where the Hall parameter is highest (Figure 2).

DISCUSSION

The linear analysis of open-cycle outflow disk generators[6] showed that the properties of the magnetoacoustic instability are strongly dependent on the electrical conductivity, the Hall parameter and the Mach number, and that strong growth of waves is possible for Mach numbers less than, as well as greater than unity. Another important factor is the time that a perturbation is resident in the channel. Despite the increased growth time at reduced Mach numbers, wave growth is still possible since a disturbance is resident in the channel for a greater length of time.

The tendency towards improved stability through operation at Mach numbers less than one with the inflow generator (Figure 5) is partially offset by the destabilizing influence of higher temperatures along the channel than in the supersonic outflow generator. The gradient of the electrical conductivity with respect to temperature has a strong influence on the development of instabilities. Typically, a 1% fluctuation in temperature corresponds to a conductivity fluctuation exceeding 10% for the generators of interest here, and the gradient itself increases with temperature. For the inflow disk generator, it was shown that reducing the electrical conductivity in the channel by lowering the combustor temperature stabilizes the flow. A reduction of approximately 60 K from the initial design value was necessary, leading to a 2.4% reduction in enthalpy extraction.

It appears that suppression of growth of magnetoacoustic waves through altering the state of the flow can only be carried out at the expense of enthalpy extraction. In this study, stable designs have not been optimised with regard to enthalpy extraction and it may be possible to improve somewhat on the value of 16.4% attained by lowering the combustor temperature.

It may also be possible to suppress wave growth by increasing the number of electrodes, and, with the appropriate external circuitry, control fluctuations in the electric field strength. Investigation of possible stabilization of the supersonic outflow disk generator using multiple electrodes and load circuits has shown that such an approach is not effective if the number of additional electrodes is small enough to be considered practical. However, growth times are much longer for the subsonic inflow disk design than the outflow design, and, in the case of the inflow disk, a relatively small change in the initial operating condition leads to stabilization of the generator. Thus it is possible that the inflow design may be stabilized by the addition of control electrodes, and this requires further investigation.

The parameters used in this analysis are typical of those employed in the modelling of large-scale open-cycle MHD generators. From this study, and the previous studies of disk generators, it is evident that questions of stability must be taken into account if either the inflow or outflow geometries are to be considered for base-load power generation.

REFERENCES

1. Nakamura, T. and Jenkins, M.K., "Performance of Disk Generators for Open-Cycle MHD Power Generation", *Journal of Energy*, Vol. 3, July-Aug. 1979, pp. 217-226.

2. Nakamura, T., Lear, W.E., and Eustis, R.H., "Inflow Disk Generator for Open-Cycle Power Generation", *Journal of Energy*, Vol. 7, Jan-Feb., 1983, pp. 29-42.

3. Simpson, S.W., Marty, S.M., and Messerle, H.K., "Open-Cycle Disk MHD Generators: Laboratory Experiments and Predictions for Base-Load Operation", *Magnetohydrodynamics*, Vol. 2, 1989, pp. 57-63.

4. Locke, E.V. and McCune, J.E., "Growth Rates for Axial Magnetoacoustic Waves in a Hall Generator", *AIAA Journal*, Vol. 4, Oct. 1966, pp. 1748-1751.

5. Fishman, F.J., "Instability of Hall MHD Generators to Magnetoacoustic Waves", *AIAA Journal*, Vol. 8, Apr. 1970, pp 632-639.

6. Marty, S.M., Simpson, S.W. and Messerle, H.K., "Stability of Open-Cycle Disk Generators," 26th Symposium on Engineering Aspects of MHD, Nashville, Tennessee, 1988, pp. 7.4.1-7.4.11

7. Marty, S.M., Simpson, S.W. and Messerle, H.K., "Two-Dimensional Analysis of Open-Cycle Disk Generators Stability", Tenth International Conf. on MHD Electrical Power Generation, Tiruchirapalli, India, 1989, pp X.59-X.62.

8. Retallick, F.D., "Disk MHD Generator Study", NASA Report CR-159872, 1980.

9. Roache, P.J., *Computational Fluid Dynamics*, Hermosa Publishers, Albuquerque, 1972.

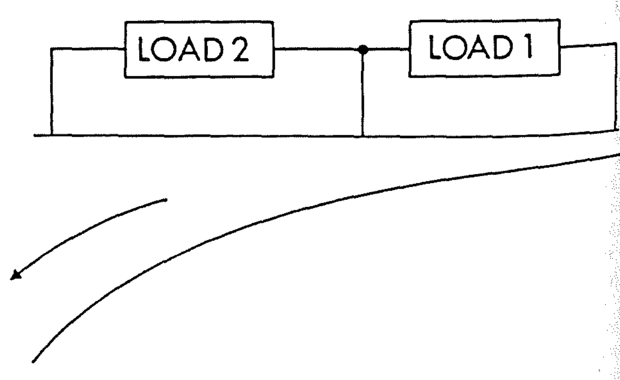

Figure 1. Configuration of radial inflow generator with two load circuits.

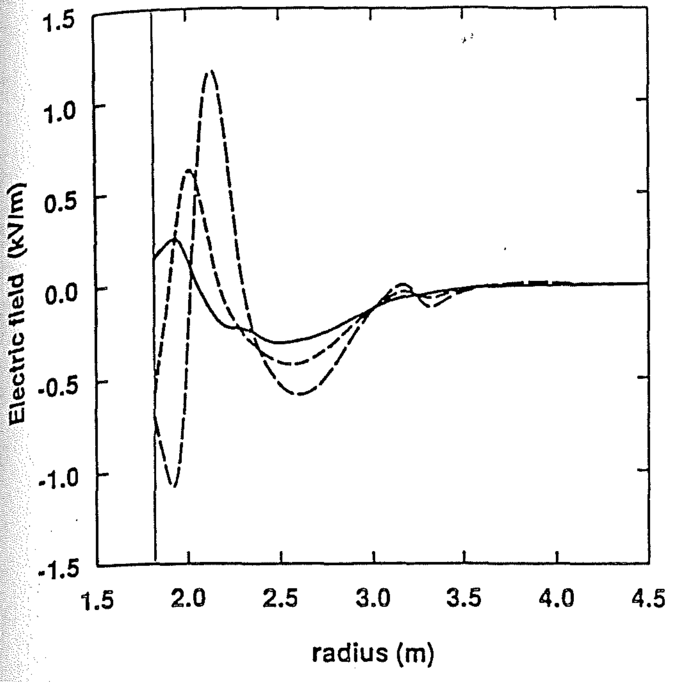

Figure 2. Difference in electric field strength from its value at t=0 versus radius at times of 2, 3 and 4 msec. The vertical line shows the location of the inner electrode. The intermediate electrode is located at a radius of 3.0 m.

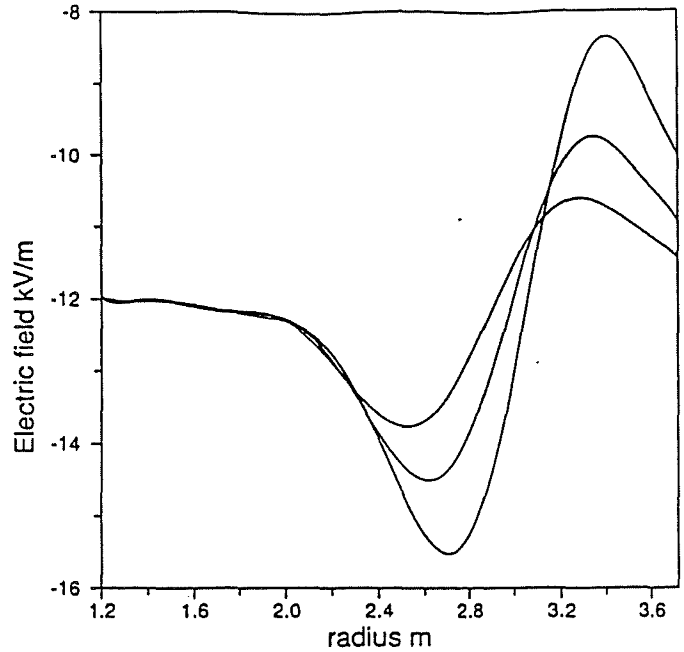

Figure 4. Mach number versus radius at times of 0, 10, 20, 30 and 40 msec for the inflow disk generator. The current in load circuit 2 (Fig. 1) is perturbed 0.5% below the design value.

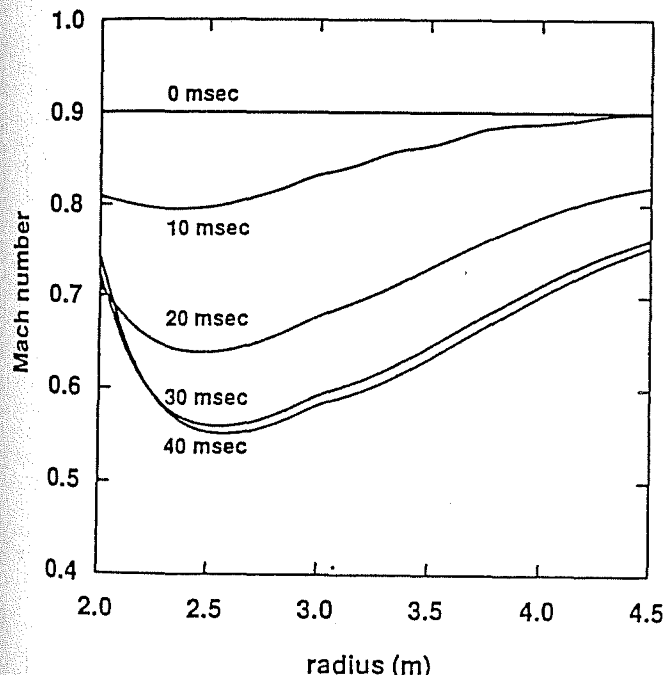

Figure 3. Electric field strength versus radius for the supersonic radial-outflow disk generator at times of 2.2, 2.4 and 2.6 msec.[6] Design parameters are comparable to those of the inflow generator (see Figure 2).

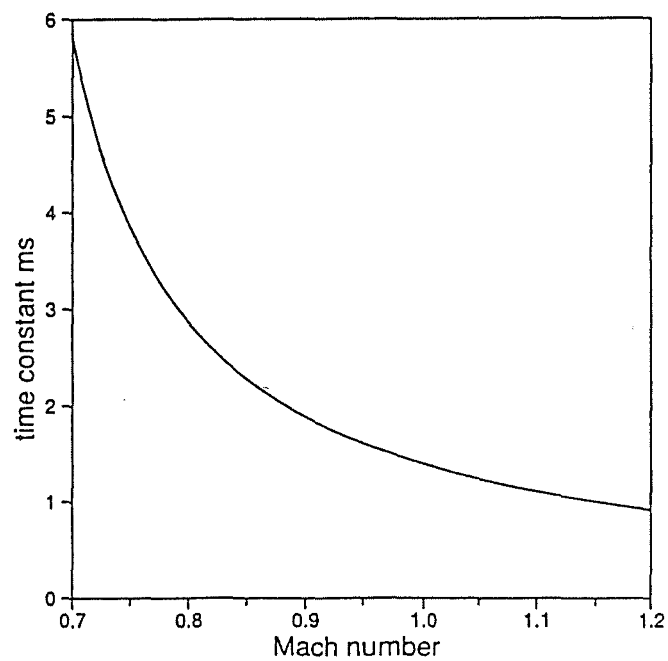

Figure 5. Growth time constant for magnetoacoustic waves versus Mach number. Properties of the inflow generator at the channel mid-radius were used for the calculation.

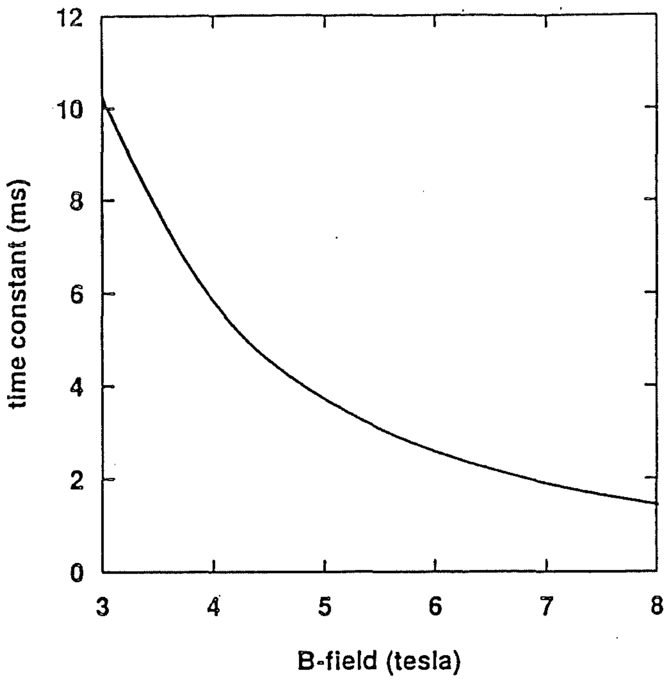

Figure 6. Growth time constant versus magnetic field strength for the inflow generator. Properties of the inflow generator at the channel mid–radius were used for the calculation.